Supporting Information

Structural Changes Induced by the Promoter Ga in Nanocrystalline ZnO Support Used in Methanol Catalysis

Jan Konrad Wied[‡[a]], Benjamin Mockenhaupt[‡[b]], Sebastian Mangelsen[c], Ulrich Schürmann[d], Lorenz Kienle[d], Malte Behrens[c]* and Jörn Schmedt auf der Günne*[a]

[a] University of Siegen, Faculty IV: School of Science and Technology, Department for Chemistry and Biology, Inorganic Materials Chemistry and Center of Micro- and Nanochemistry and Engineering (Cμ), Adolf-Reichwein Straße 2, 57076 Siegen, Germany.

[b] University of Duisburg-Essen, Technical Chemistry 1, Universitätsstr. 7, 45141 Essen, Germany.

[c] Kiel University, Institute of Inorganic Chemistry, Max-Eyth-Straße 2, 24118 Kiel, Germany.

[d] Kiel University, Department of Materials Science, Kaiserstraße 2, 24143 Kiel, Germany.

‡ These authors contributed equally.

* Corresponding authors: E-mail: mbehrens@ac.uni-kiel.de, gunnej@chemie.uni-siegen.de

Content:

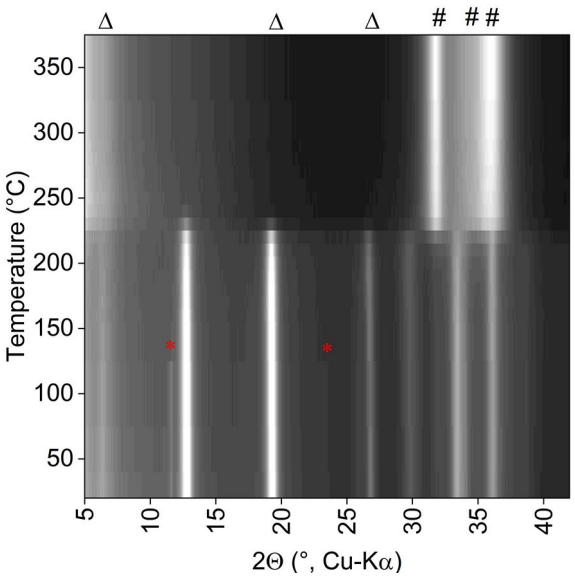

Fig. S1: Temperature-resolved PXRD analysis of the thermal decomposition of the hydrozincite precursor containing 15% gallium (x_{Ga} = 0.15). The PXRD analysis was performed in static air. The reflection positions are labeled as followed: zaccagnaite-like side phase (*), ZnO (#) and additional reflections (Δ), all others hydrozincite.

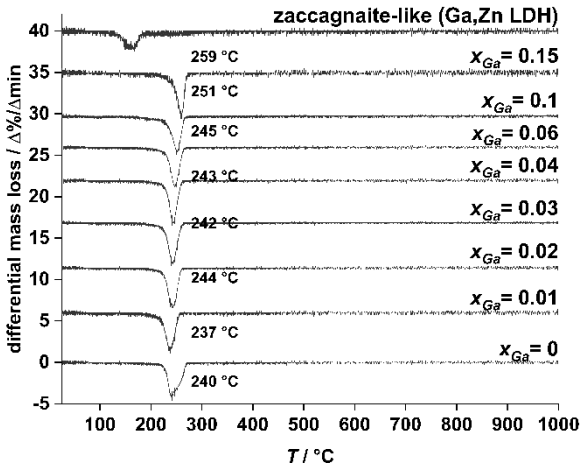

Fig. S2: Differential plot of the thermogravimetric analysis of the decomposition of the hydrozincite precursors in synthetic air into zinc oxide in comparison to the synthesized zaccagnaite-like Ga,Zn LDH. The labeled temperatures correspond to the minimum. x_{Ga} is the metal-based fraction.

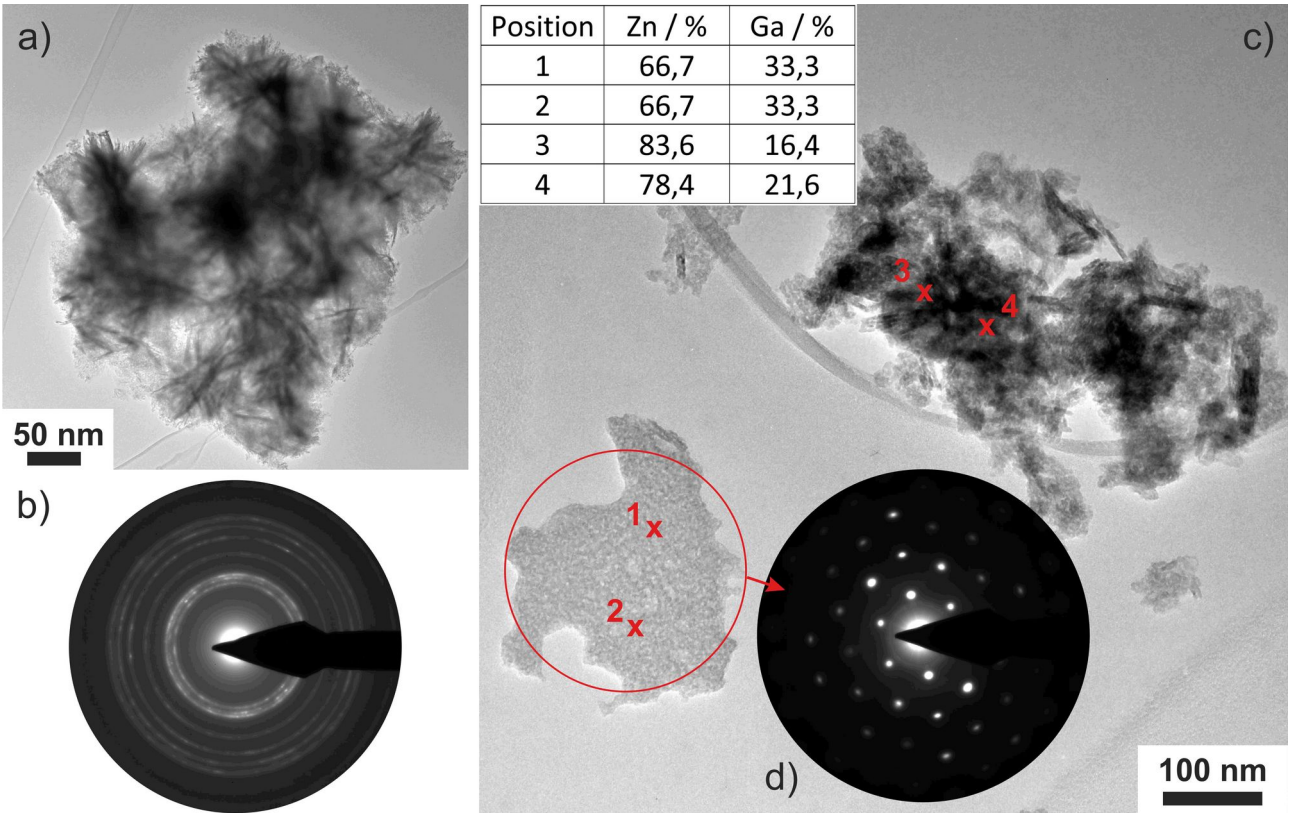

Position	Zn / %	Ga / %
1	66,7	33,3
2	66,7	33,3
3	83,6	16,4
4	78,4	21,6

Fig. S3: a) TEM overview image and b) corresponding electron diffraction pattern of a medium Ga doped ZnO (x_{Ga} = 0.04). c) TEM overview image with different morphologies of a heavy Ga doped ZnO (x_{Ga} = 0.15). Crosses mark positions of EDX point measurements with the Zn and Ga fractions in inserted the table. d) Electron diffraction pattern of a single crystalline flake with high Ga content.

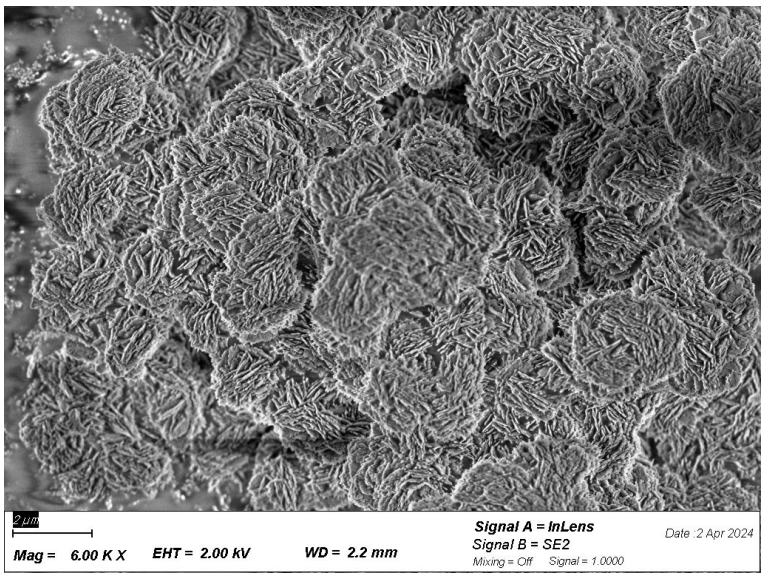

Fig. S4: SEM image of gallium doped hydrozincite with x_{Ga} = 0.03, exhibiting a platelet morphology.

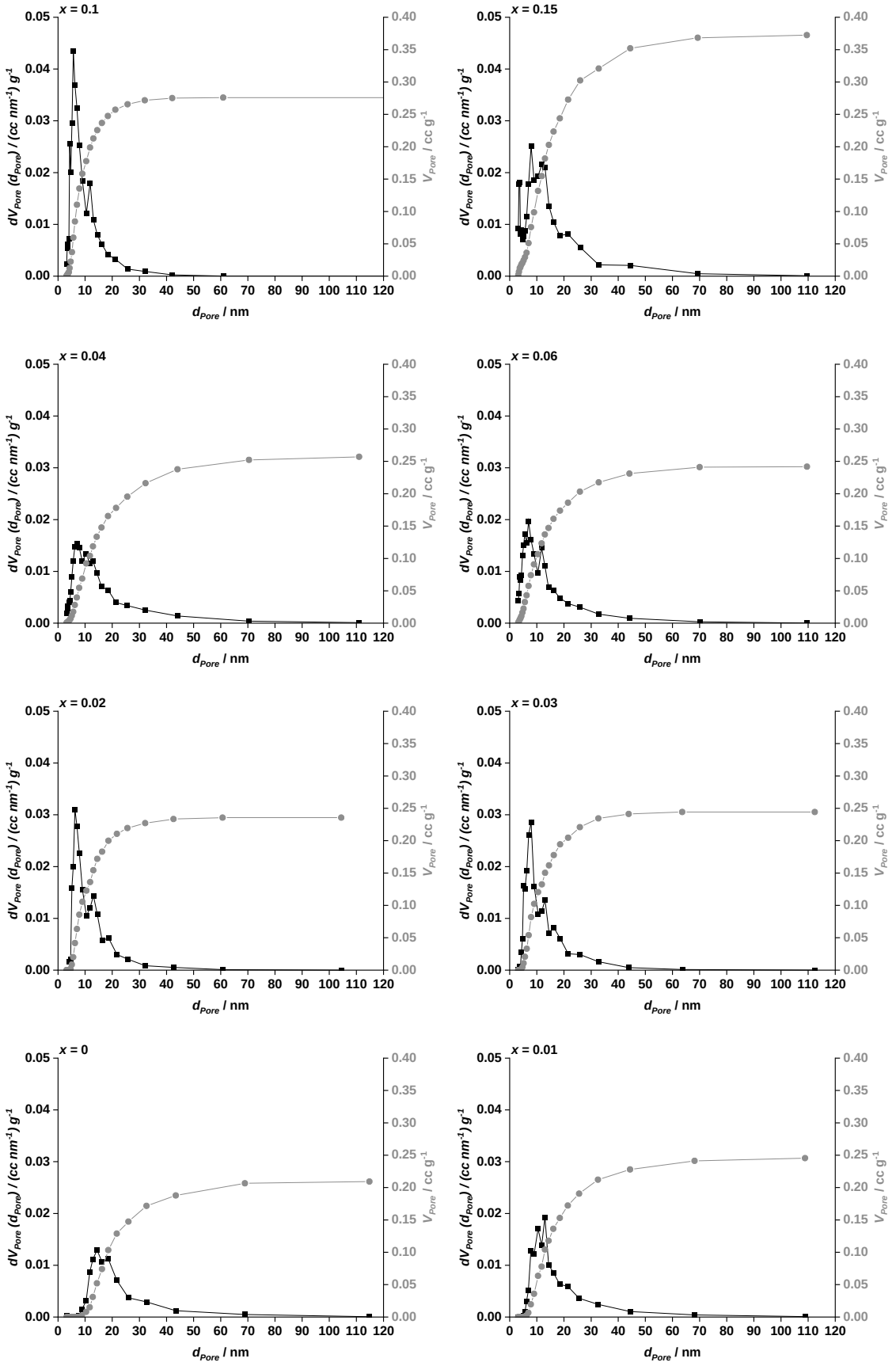

Fig. S5: Pore size and pore volume distribution for the gallium doped zinc oxides. The calculation was performed on the desorption isotherm by BJH method.

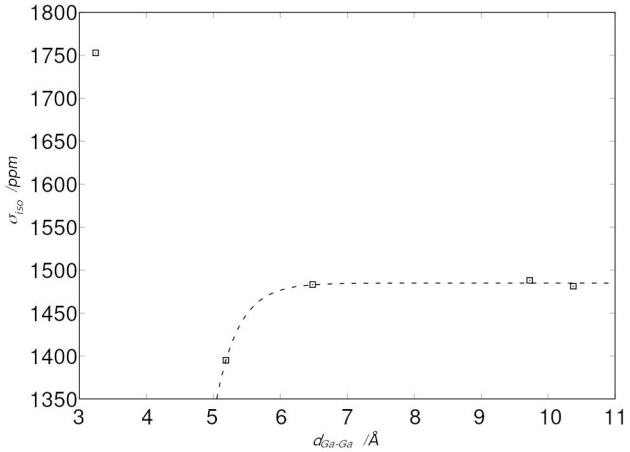

Fig. S6: Isotropic chemical shielding σ_{iso}^{calc} convergence plot for the $Ga_{i;Tetra}^{\bullet\bullet\bullet}$ defect, resulting in an isotropic chemical shielding value of 1484.7 ± 3.5 ppm extrapolated to an infinitely large supercell. Plotted are the isotropic chemical shielding σ_{iso}^{calc} values against the shortest Ga-Ga distance in the different supercell, $d_{Ga\text{-}Ga}$. The isotropic chemical shielding σ_{iso}^{calc} values for the different sized supercells are shown in Tab. S2.

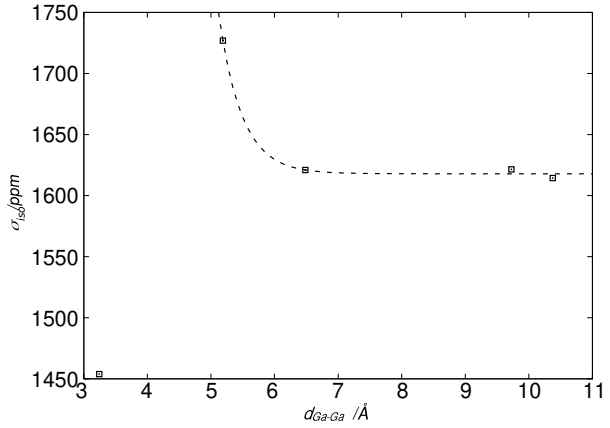

Fig. S7: Isotropic chemical shielding σ_{iso}^{calc} convergence plot for the $Ga_{i;Octa}^{\bullet\bullet\bullet}$ defect, resulting in an isotropic chemical shielding value of 1617.9 ± 3.6 ppm extrapolated to an infinitely large supercell. Plotted are the isotropic chemical shielding σ_{iso}^{calc} values against the shortest Ga-Ga distance in the different supercell, $d_{Ga\text{-}Ga}$. The isotropic chemical shielding σ_{iso}^{calc} values for the different sized supercells are shown in Tab. S2.

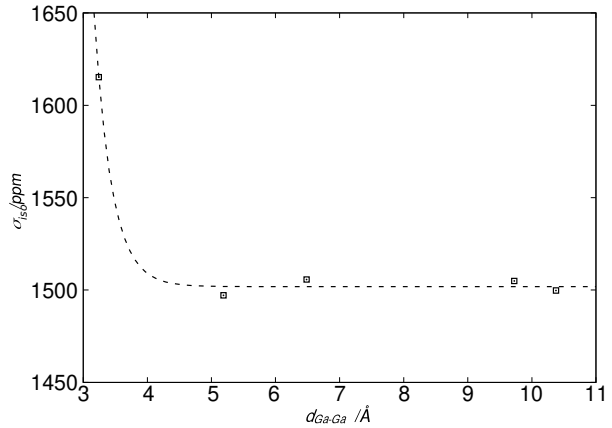

Fig. S8: Isotropic chemical shielding σ_{iso}^{calc} convergence plot for the $[Ga_{Zn}^{\bullet}+V_{Zn}^{''}]$ defect, resulting in an isotropic chemical shielding value of 1501.9 ± 2.9 ppm extrapolated to an infinitely large supercell. Plotted are the isotropic chemical shielding σ_{iso}^{calc} values against the shortest Ga-Ga distance in the different supercell, $d_{Ga\text{-}Ga}$. The isotropic chemical shielding σ_{iso}^{calc} values for the different sized supercells are shown in Tab. S2.

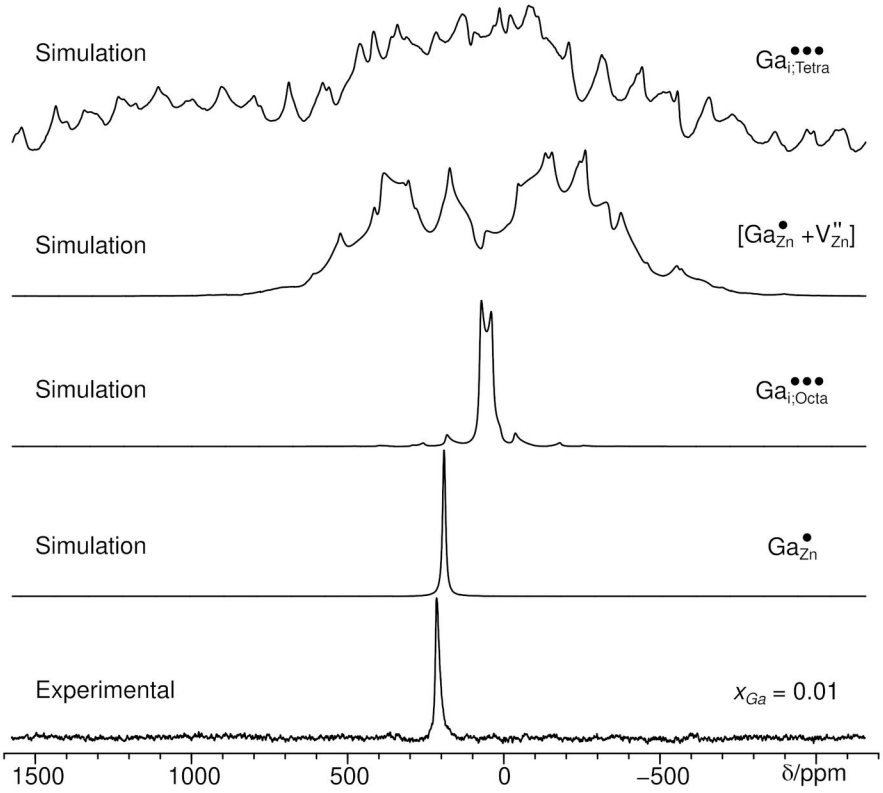

Fig. S9: ^{71}Ga MAS NMR stackplot showing the experimentally measured spectrum of the ZnO:Ga sample with a gallium content of x_{Ga} = 0.01, as well as simulations for the $Ga_{Zn}^{\bullet}$, $Ga_{i;Octa}^{\bullet\bullet\bullet}$, $Ga_{i;Tetra}^{\bullet\bullet\bullet}$ and $[Ga_{Zn}^{\bullet}+V_{Zn}^{''}]$ gallium containing defects. All spectra were acquired at a spinning frequency of 20 kHz.

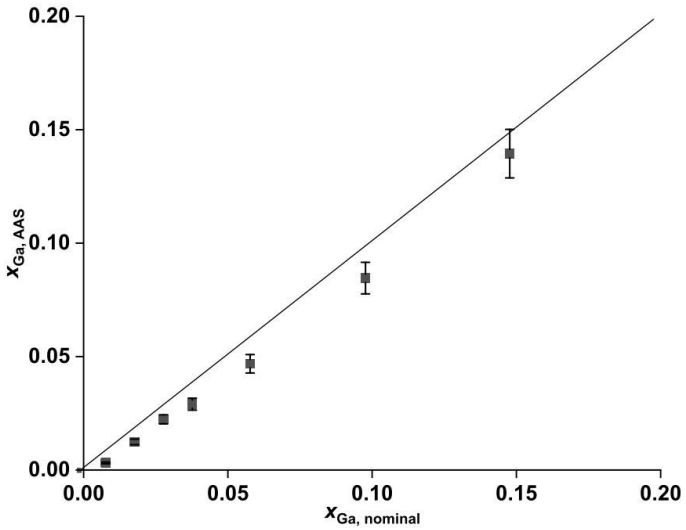

Fig. S10: Nominal and measured Ga substitution ratio x_{Ga} determined by ICP/AAS analysis of the ZnO:Ga materials. The line indicates the expected correlation. Atomic absorption spectroscopy was performed on a Thermo Fisher iCE-3500 AAS after dissolving the doped hydrozincite sample in nitric acid overnight. A strong linear correlation between nominal and observed ratios can be observed, while the measured content is systematically lower as expected which reflects errors in sample preparation for example by the starting agents like $Ga(NO_3)_3$ forming hydrates under ambient conditions.

Table S1: List of the chemicals and their purity used for co-precipitation.

Chemicals	Supplier	Purity
$Zn(NO_3)_2 \cdot 6\ H_2O$	Carl Roth GmbH + Co. KG	≥ 99 %
$Ga(NO_3)_3 \cdot x\ H_2O$	Alfa Aesar	≥ 99 %

The water content in the gallium salt was determined by TGA analysis, considering the total oxidation of $Ga(NO_3)_3$ to Ga_2O_3.

Tab. S2: List of reference compounds used for the generation of an isotropic chemical shielding σ_{iso}^{calc} into isotropic chemical shift δ_{iso}^{pred} conversion formula as well as a quadrupolar coupling constant C_Q^{calc} into C_Q^{pred} conversion formula. Listed are the used structure files with their ICSD collection number, the coordination of the gallium atoms inside the structure, the isotropic chemical shielding σ_{iso}^{calc} and isotropic chemical shift δ_{iso}^{exp} values, the quadrupolar coupling constants C_Q^{calc} and C_Q^{exp} and the asymmetry η_Q^{pred} parameter. The structure file for $LaGaGe_2O_7$ was generated by an isostructural transformation using a model from the $LaAlGe_2O_7$ crystal structure[1] and a variable-cell relaxation using the Quantum-Espresso software.

Compound	Structure file (ICSD-No.)	Coordination	δ_{iso}^{exp} /ppm	σ_{iso}^{calc} /ppm	C_Q^{exp} / MHz	C_Q^{calc} / MHz	η_Q^{pred}	Ref.
α-Ga_2O_3	27431	GaO_6	56	1652.26	8.2	6.2	0.08	[2]
β-Ga_2O_3	144115	GaO_6	25	1663.33	8.3	5.1	0.08	[3]
		GaO_4	198	1487.71	11	8.4	0.85	
$LiGaO_2$	18152	GaO_4	242	1462.92	3.89	3.89	0.37	[2]
$NaGaO_2$	36652	GaO_4	238	1466.64	3.69	3.69	0.40	[2]
$Ga_2(SO_4)_3$	79304	GaO_6	-87	1806.38	0.0	0.0	0.00	[2]
		GaO_6	-98	1827.33	1.9	1.2	0.20	
GaN	34476	GaN_4	333	1363.61		1.1		[4]
GaP	635040	GaP_4	307	1376.3		0.0		[4]
$ZnGa_2O_4$	237886	GaO_6	80	1627.45	6.78	1.8	0.00	[5]
$GaPO_4$-quartz	30881	GaO_4	100.3	1614.33	8.6	6.1	0.51	[3]
$GaPO_4$-cristobalite	97550	GaO_4	118	1610.77	4.7	3.6	0.45	[3]
$LaGaO_3$	41280	GaO_6	56.1	1667.44	1.30	1.1	0.50	[2]
$Y_3Ga_5O_{12}$	80148	GaO_6	5.6	1707.24	4.1	6.1	0.03	[3]
		GaO_4	219	1475.36	13.1	12.4	0.05	
$KGaO_2$	9009	GaO_4	225	1481.53	3.5	3.1	0.40	[2]
		GaO_4	232	1479.12	3.6	3.2	0.60	
$LaGaGe_2O_7$		GaO_5	75.8	1637.19	15.0	12.4	0.70	[3]

Tab. S3: List of the isotropic chemical shielding values, σ_{iso}^{calc}, the quadrupolar coupling constant C_Q^{calc} and the quadrupolar asymmetry parameter η_Q^{pred} for different supercell sizes with different point-defect distances, $d_{Ga\text{-}Ga}$, for the investigated defects $Ga_{Zn}^{\bullet}$, $Ga_{i;Octa}^{\bullet\bullet\bullet}$, $Ga_{i;Tetra}^{\bullet\bullet\bullet}$ and $[Ga_{Zn}^{\bullet}+V_{Zn}^{''}]$.

Defect	Supercell	$d_{Ga\text{-}Ga}$ /A	σ_{iso}^{calc} /ppm	C_Q^{calc} / MHz	η_Q^{pred}
$Ga_{Zn}^{\bullet}$	1x2x2	3.2417	1696.64	-9.1	0.0
	2x2x1	5.1876	1552.88	0.2	0.0
	3x2x2	6.4834	1516.69	1.3	0.7
	3x3x2	9.7251	1508.95	1.4	0.0
	4x4x2	10.3752	1502.25	1.7	0.0
$Ga_{i;Octa}^{\bullet\bullet\bullet}$	1x2x2	3.2417	1453.84	-15.9	0.5
	2x2x1	5.1876	1726.90	12.3	0
	3x2x2	6.4834	1621.20	-6.7	0.3
	3x3x2	9.7251	1621.51	8.3	0
	4x4x2	10.3752	1614.40	5.4	0
$Ga_{i;Tetra}^{\bullet\bullet\bullet}$	1x2x2	3.2417	1752.02	-4.3	0.5
	2x2x1	5.1876	1395.03	-15.4	0.5
	3x2x2	6.4834	1483.18	-11.2	0.7
	3x3x2	9.7251	1488.05	-18.1	0.8
	4x4x2	10.3752	1481.11	-18.6	0.7
$[Ga_{Zn}^{\bullet}+V_{Zn}^{''}]$	1x2x2	3.2417	1614.58	8.6	0.6
	2x2x1	5.1876	1497.15	-14.7	0.8
	3x2x2	6.4834	1505.66	-12.0	0.7
	3x3x2	9.7251	1504.93	-12.1	0.4
	4x4x2	10.3752	1499.75	-12.6	0.4

References

[1] S. C. Adediwura, J. K. Wied, C. F. Litterscheid, M. R. Kontham, L. P. Rüthing, J. Schmedt auf der Günne, manuscript in preparation **2025**.

[2] J. T. Ash, P. J. Grandinetti, *Magn. Reson. Chem.* **2006**, *44*, 823–831.

[3] D. Massiot, T. Vosegaard, N. Magneron, D. Trumeau, V. Montouillout, P. Berthet, T. Loiseau, B. Bujoli, *Solid State Nucl. Magn. Reson.* **1999**, *15*, 159–169.

[4] O. H. Han, H. K. C. Timken, E. Oldfield, *J. Chem. Phys.* **1988**, *89*, 6046.

[5] M. Allix, S. Chenu, E. Veron, T. Poumeyrol, E. A. Kouadri-Boudjelthia, S. Alahrache, F. Porcher, D. Massiot, F. Fayon, *Chem. Mater.* **2013**, *25*, 1600–1606.